

Accepted Manuscript

Title: Miniature photonic crystal cavity sensor for simultaneous measurement of liquid concentration and temperature

Author: Ya-nan Zhang Yong Zhao Hai-feng Hu



PII: S0925-4005(15)00546-8
DOI: <http://dx.doi.org/doi:10.1016/j.snb.2015.04.094>
Reference: SNB 18399

To appear in: *Sensors and Actuators B*

Received date: 26-2-2015
Revised date: 11-4-2015
Accepted date: 18-4-2015

Please cite this article as: Y.-n. Zhang, Y. Zhao, H.-f. Hu, Miniature photonic crystal cavity sensor for simultaneous measurement of liquid concentration and temperature, *Sensors and Actuators B: Chemical* (2015), <http://dx.doi.org/10.1016/j.snb.2015.04.094>

This is a PDF file of an unedited manuscript that has been accepted for publication. As a service to our customers we are providing this early version of the manuscript. The manuscript will undergo copyediting, typesetting, and review of the resulting proof before it is published in its final form. Please note that during the production process errors may be discovered which could affect the content, and all legal disclaimers that apply to the journal pertain.

Miniature photonic crystal cavity sensor for simultaneous measurement of liquid concentration and temperature

Ya-nan Zhang¹, Yong Zhao^{1,2,*}, Hai-feng Hu¹

¹ College of Information Science and Engineering, Northeastern University, Shenyang 110819, China

² State Key Laboratory of Synthetical Automation for Process Industries, Shenyang 110819, China

**Corresponding author: zhaoyong@ise.neu.edu.cn*

Abstract

A new method for simultaneous measurement of liquid concentration and temperature is proposed by using a miniature photonic crystal sensor, where two cascaded cavities (H0 cavity and H1 cavity) are separately located adjacent to one waveguide. The standard liquid whose concentration is fixed and known will be infiltrated in defected holes of the H1 cavity, and the measured liquid whose concentration is unknown will be infiltrated in defected holes of the H0 cavity. Both the two independent resonant dips of cascaded cavities that can be simultaneously monitored at output spectrum of the waveguide will shift with the variation of liquid concentration or ambient temperature. By using finite difference time domain (FDTD) simulation, resonant properties of the two cavities are respectively optimized, and then the linear relationships between shifts of two resonant dips and liquid concentration/temperature are calculated. Finally, according to dual-wavelength matrix method, liquid concentration measurement with a resolution of 9.4322 ppm and temperature measurement with a resolution of 0.0136 K are simultaneously realized, which can not only solve the cross-sensitivity problem between liquid concentration and temperature, but also provide a solution for two-parameter measurement in a miniaturized system.

Keywords: Liquid concentration measurement; temperature measurement; simultaneous measurement; miniature sensor; photonic crystal cavity

1. Introduction

Liquid concentration, as a main physicochemical parameter of target liquid, has attracted considerable attention in the application fields of fundamental research, biochemical analysis, medical diagnosis, environmental assessment, chemical industry, and so on [1, 2]. Naturally, many methods have been developed to measure this parameter [3-6]. Among them, refractive index (RI) sensor is the most popular apparatus due to that RI variation of liquid is directly related to concentration or existence of target liquid and the target liquid can be detected in its natural form without any modifications [6]. Particularly, optical RI sensor inherits the peculiar advantages of optical fiber sensing techniques, such as immunity to electromagnetic interference, safety in flammable explosive environment, rapid response speed, and the ability of remote on-line sensing [6-8]. However, now the commercially available optical RI sensors usually have a relatively large sensing probe, and thus greatly limit their applications in the case that only a limited amount of liquid sample can be supplied. Therefore, it is particular important to develop miniaturized optical RI sensor, which is beneficial in realizing portable, low cost, and low power detection of liquid concentration with rapid analysis time and reduced liquid consumption.

On the other hand, it has been demonstrated that photonic crystal (PC), which is formed by periodically arranging regularly shaped materials with different dielectric constants in a substrate, presents the capability of guiding and manipulating light at the scale of optical wavelength [9]. Besides, the periodic air hole of hole-typed PC is a natural candidate for housing target liquid, and the inner variations of holes will bring much more strong influences on propagating light. Particularly, PC cavity, which is formed by introducing some intentional point defects in the PC, exhibits strong field confinement in the defected region and has long photon lifetime (namely,

high Q) [10]. These characteristics will further enhance the light-liquid interaction and give rise to an optical mode whose resonant wavelength is highly sensitive to local RI perturbations of defected holes. At present, PC cavity has been demonstrated as a promising building block for realizing miniature and high-sensitive optical RI sensor [11, 12]. In addition, PC cavity with small sensing area ($< 10 \mu\text{m}^2$) only requires about 1 fL target liquid [13]. Comparing with traditional optical RI sensor, the size of PC cavity based RI sensor can be drastically reduced. Therefore, many optical RI sensors based on PC cavity have been proposed and utilized to monitor the concentration variations of NaCl solution [14], DNA biomolecule [15], Rat monoclonal Ab [16], Human Papillomavirus virus-like particles [17], avidin [18], and so on. However, all of these presented studies had not considered the influence of temperature fluctuation in practical measurements. Actually, as the RI of target liquid is also related to external temperature [19-22], the measurement accuracy of liquid concentration will be easily interrupted by temperature for individual RI sensor. Therefore, it is necessary to discriminate or compensate for the influence of temperature when the PC cavity based RI sensor is used for concentration measurement [21]. Furthermore, it is much more desirable to simultaneously measure liquid concentration and temperature in many applications [22-25]. Recently, we have demonstrated that a cascaded cavity slab can be used to simultaneously measure magnetic field and temperature with high sensitivity and small size [20], in which the two cavities were considered to be absolutely independent. Absolutely, this hypothesis is just an extreme scenario and will bring some slight measurement errors. Besides, the wavelength spacing between the two cascaded cavities is a bit narrow and the quality factors of two cavities are too low, which will limit the measurement range of sensor and even cause the crosstalk between two measured signals.

In this paper, a novel cascaded PC cavity sensor with wider wavelength spacing is proposed. Besides, this miniaturized and high-sensitive sensor can be well used for simultaneous measurement of liquid concentration and temperature. Taking NaCl-H₂O solution as an example, the measurement principle with considering the cross influences of two cavities is described, and the structural design of two PC cavities are explained. Finally, the sensing properties of the proposed cascaded PC cavity are analyzed.

2. System Design and Working Principle

A schematic configuration of the proposed PC cavity sensor is shown in Fig. 1(a). Here, the light source is an amplified spontaneous emission (ASE) with central wavelength of 1550 nm, spectral width of 100 nm, and output power of 30 mW. After light beam went through the cascaded PC cavity, it will be transmitted into an optical spectrum analyzer (OSA) to monitor transmission spectrum of the PC cavity. Besides, all of these optical instruments are linked by single mode fiber (SMF). Fig. 1(b) presents the specific structure of PC cavity, where one H0 cavity (on the right) and one H1 cavity (on the left) are located adjacent to one waveguide to form a cascaded cavity on one PC slab. The standard liquid whose concentration is fixed and known will be infiltrated in some holes around H1 cavity, and the measured liquid whose concentration is needed to be measured will be infiltrated in some holes around H0 cavity. Thus, the transmission spectrum of the proposed cascaded PC cavity exhibits two dips at corresponding resonant wavelengths of two different cavities.

In this work, the basic measurement principle is that the RI n of liquid that infiltrated in the air holes of PC cavity is a function of its concentration C and ambient temperature T [22, 25]. When C or T changes, the RI n will also change and can be expressed as [25]:

$$\Delta n = \frac{\partial n}{\partial C} \Delta C + \frac{\partial n}{\partial T} \Delta T = K_C \Delta C + K_T \Delta T \quad (1)$$

where $K_C = \partial n / \partial C$ and $K_T = \partial n / \partial T$ represent the RI sensitivities of liquid to the concentration and temperature, respectively. According to the past studies on the relation between the RI of liquid and its concentration, K_C is a fixed value for certain liquid under different temperatures, and so does K_T for certain liquid under different liquid concentrations. Namely, the values of K_C and K_T are only related to the type of liquid, and they are fixed once the type of liquid is definite.

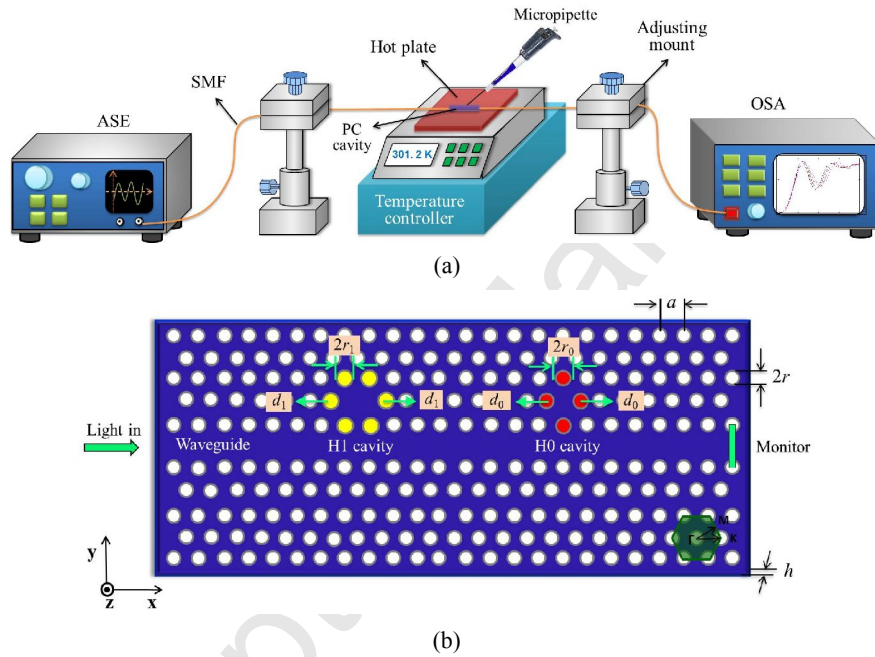


Fig. 1. (a) Schematic structure of liquid concentration/temperature sensor based on PC cavity; (b) Specific structure of PC slab, where one H0 cavity and one H1 cavity are cascaded together.

For the standard liquid that infiltrated in the H1 cavity, its RI variation Δn_1 is only related to the disturbance of ambient temperature ΔT . While for the measured liquid that infiltrated in the H0 cavity, its RI variation Δn_0 is related to both the concentration change of measured liquid ΔC and the disturbance of ambient temperature ΔT . Therefore, the RI variations of the two infiltrated liquids can be described in a matrix as follows:

$$\begin{pmatrix} \Delta n_0 \\ \Delta n_1 \end{pmatrix} = \begin{pmatrix} K_{C0} & K_{T0} \\ 0 & K_{T1} \end{pmatrix} \begin{pmatrix} \Delta C \\ \Delta T \end{pmatrix} \quad (2)$$

where, K_{C0} is the RI sensitivity of the measured liquid to concentration; K_{T0} and K_{T1} are the RI

sensitivities of the measured liquid and the standard liquid to temperature. Then, the wavelength shift of H0 cavity $\Delta\lambda_0$ and the wavelength shift of H1 cavity $\Delta\lambda_1$ can be expressed as:

$$\begin{pmatrix} \Delta\lambda_0 \\ \Delta\lambda_1 \end{pmatrix} = \begin{pmatrix} S_{00} & S_{01} \\ S_{10} & S_{11} \end{pmatrix} \begin{pmatrix} \Delta n_0 \\ \Delta n_1 \end{pmatrix} = \begin{pmatrix} S_{00}K_{C0} & S_{00}K_{T0}+S_{01}K_{T1} \\ S_{10}K_{C0} & S_{10}K_{T0}+S_{11}K_{T1} \end{pmatrix} \begin{pmatrix} \Delta C \\ \Delta T \end{pmatrix} \quad (3)$$

where, S_{00} and S_{10} are respectively the wavelength sensitivities of first cavity and second cavity to the RI of measured liquid, while S_{01} and S_{11} are respectively the wavelength sensitivities of first cavity and second cavity to the RI of standard liquid. The four sensitivity values are determined by the resonant properties of the two PC cavities. Therefore, the concentration of measured liquid and temperature can be deduced by:

$$\begin{pmatrix} \Delta C \\ \Delta T \end{pmatrix} = \begin{pmatrix} S_{00}K_{C0} & S_{00}K_{T0}+S_{01}K_{T1} \\ S_{10}K_{C0} & S_{10}K_{T0}+S_{11}K_{T1} \end{pmatrix}^{-1} \begin{pmatrix} \Delta\lambda_0 \\ \Delta\lambda_1 \end{pmatrix} \quad (4)$$

From Eq. (4), it can be concluded that the concentration of measured liquid and temperature can be simultaneously measured by monitoring the wavelength shifts of first cavity and second cavity. Besides, the measurement sensitivities of liquid concentration and temperature are not only determined by the RI sensitivities of liquid to concentration and to temperature, whose values are fixed when the type of liquid that infiltrated in PC cavities is fixed, but also related to the wavelength sensitivities of cavities to corresponding RI variations, which depend on the structural configurations of the two PC cavities. Therefore, this work will focus on the structural optimizations of the two PC cavities, in which the main aim is to enhance S_{00} , S_{10} , S_{01} , and S_{11} , and thus improve the measurement sensitivities of both liquid concentration and temperature.

3. Model and Optimization of PC Cavity

As shown in Fig. 1(b), the proposed PC cavity slab is constructed by arranging air holes of triangular lattice on a silicon slab ($n_{\text{si}}=3.48$) of silicon-on-insulator (SOI) substrate. The air holes in the central row of triangular lattice PC are removed to form a W1 PC waveguide (PCW). And

to form cascaded PC cavity, some holes in the second row adjacent to the waveguide will be modified according to the following procedures: first, adjusting the radii of the two red-colored air holes (defected holes) and shifting them away from each other to realize an optimized H0 cavity that side-coupled to the PCW; then, removing one air hole and adjusting the radii and positions of the two yellow-colored air holes (defected holes) adjacent to this empty hole to realize an optimized H1 cavity that side-coupled to the PCW. It has been demonstrated that the two side-coupled PC cavities possess a better coupling between the PCW and the defects [26]. In this design, the lattice constant is $a=440$ nm, the radius of bulk air hole is $r=0.3a=132$ nm, and the thickness of the PC slab is $h=0.5a=220$ nm. The radius and shifting distance of defected holes in H0 cavity are defined as r_0 and d_0 , respectively. Similarly, the radius and shifting distance of defected holes in H1 cavity are defined as r_1 and d_1 , respectively. Particularly, the RI of all defected holes (four red-colored holes and six yellow-colored holes) is temporarily set as 1.33.

Maintaining high quality factor (Q) is desirable since it can enhance the interaction between target liquid and optical field, which will then improve the wavelength sensitivity of cavity to RI variation. At the same time, it will reduce the line-width of resonant spectrum, which enables a low crosstalk of the two cavities in the same PC slab [27]. Therefore, in the following we will optimize the structures of H0 cavity and H1 cavity, respectively, to increase their Q values, and thus improve the corresponding properties of the whole sensing system. The properties of PC cavities are numerically analyzed by finite difference time domain (FDTD) method with using MIT's freely available software Meep [28]. In the following numerical simulations, effective RI of 2.87 is used for 220 nm thick silicon slab [29, 30]. We restrict our calculations to TE-polarization mode, namely, the electric field is parallel to the plane of PC slab. For all simulations, the time

step is set to be 2000 with resolution of 10, and the entire simulation space is surrounded by perfectly matched layer with thickness of $1.0a$, absorbing any fields leaving at the boundaries of simulation region in order to prevent reflections.

3.1 Structural Optimization of H0 Cavity

In this subsection, we discuss the dependences of resonant properties of H0 cavity on the shifting distance d_0 and radius r_0 of defected holes. Fig. 2(a) presents the variations of resonance wavelength λ_0 and quality factor Q when the shifting distance d_0 is changed from $0.16a$ to $0.30a$ with an increment of $0.02a$. We can see that the resonant wavelength λ_0 shifts towards longer wavelength with the increase of shifting distance d_0 , due to the increase of high-dielectric material in the cavity region. Meanwhile, the Q factor of resonant mode changes significantly, and the shifting distance of $d_0=0.22a$ results in an optimal design at $\lambda_0=1560.88$ nm with Q factor of 2035, for which the maximum coupling strength between the H0 cavity and the PCW is achieved. Then, we will investigate the relationship between the resonant properties of H0 cavity and the radius r_0 when $d_0=0.22a$. As r_0 increases from $0.27a$ to $0.34a$ with a step of $0.01a$, the calculated resonant wavelength λ_0 and Q factor as a function of r_0 are shown in Fig. 2(b). As expected, the resonant wavelength will be pushed towards shorter wavelength as the increasing of r_0 . Besides, the Q factor obtains the maximum value of 2480 when $r_0=0.31a$. Therefore, we employ the H0 cavity with $d_0=0.22a$ and $r_0=0.31a$ as our optimized structure, which is shown in the inset of Fig. 3(a).

By using FDTD, the transmission spectrum and electric field distribution of the optimized H0 cavity are numerically calculated, as shown in Fig. 3(a) and Fig. 3(b), respectively. There is a sharp drop with resonant wavelength of 1552 in Fig. 3(a), where the extinction ratio of the well-defined single drop exceeds 17 dB. When light wavelength matches with the resonant

wavelength, the y-component of electric field (E_y) distribution of the optimized PC cavity in x-y plane is shown in Fig. 3(b), which shows that there is a significant amplification of light energy within the resonant cavity. Relative to optical field at side walls of resonant cavity, we can observe that the optical mode in innermost holes of resonant cavity strongly overlap with liquid that infiltrated in the defected holes. This causes the resonant cavity to be very sensitive to RI variation of liquid due to large strength of light-matter interaction inside them. Therefore, the proposed H0 cavity can be used for achieving high-sensitive RI sensor.

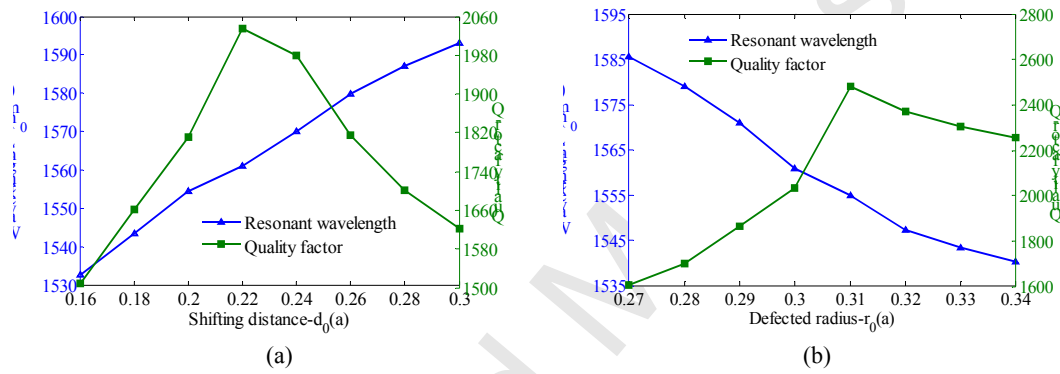


Fig. 2. Variations of resonant wavelength λ_0 and quality factor Q when the shifting distance d_0 is changed from $0.16a$ to $0.30a$ with an increment of $0.02a$ (a) and when the defected radius r_0 is changed from $0.27a$ to $0.34a$ with an increment of $0.01a$ for $d_0 = 0.22a$ (b).

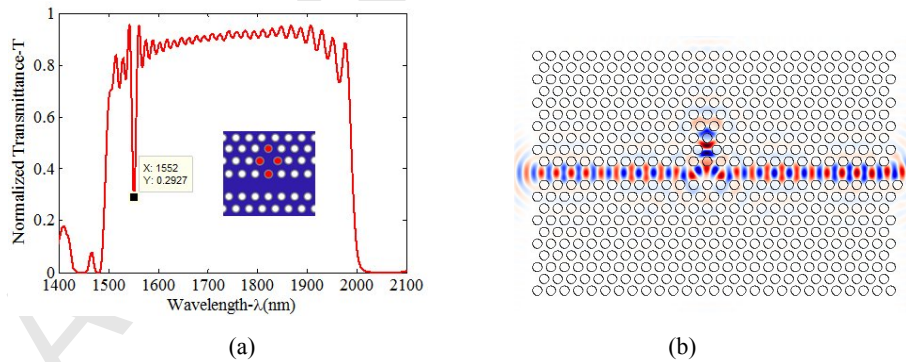


Fig. 3. Transmission spectrum (a) and electric field distribution (b) of the optimized H0 cavity with shifting distance of $0.22a$ and defected radius of $0.31a$

3.2 Structural Optimization of H1 Cavity

In this subsection, we separately discuss the dependences of resonant properties of H1 cavity on the shifting distance d_1 and radius r_1 of defected holes. Following the same optimization steps of section 3.1, we first calculate the resonant wavelength λ_1 and quality factor Q of H1 cavity when

the shifting distance d_1 is changed from $0.14a$ to $0.30a$ with an increment of $0.02a$, and then calculate the resonant wavelength λ_1 and quality factor Q when the defected radius r_1 is increased from $0.27a$ to $0.37a$ with a step of $0.01a$. From Fig. 4(a) and Fig. 4(b), we can get that the optimized H1 cavity can be obtained when $d_1=0.18a$ and $r_1=0.34a$. As seen in Fig. 5(a), this optimized H1 cavity also exist a narrow dip with resonant wavelength of 1515 nm in the transmission spectrum. The extinction ratio of the well-defined single notch exceeds 15 dB, and the calculated Q factor as high as 2230 can be observed. Therefore, we make the light wavelength match with the resonant wavelength (1515 nm), and we can get the y-component of electric field distribution of the optimized H1 cavity in x-y plane, as shown in Fig. 5(b). As seen, the light energy is strongly confined in defected region of PC cavity.

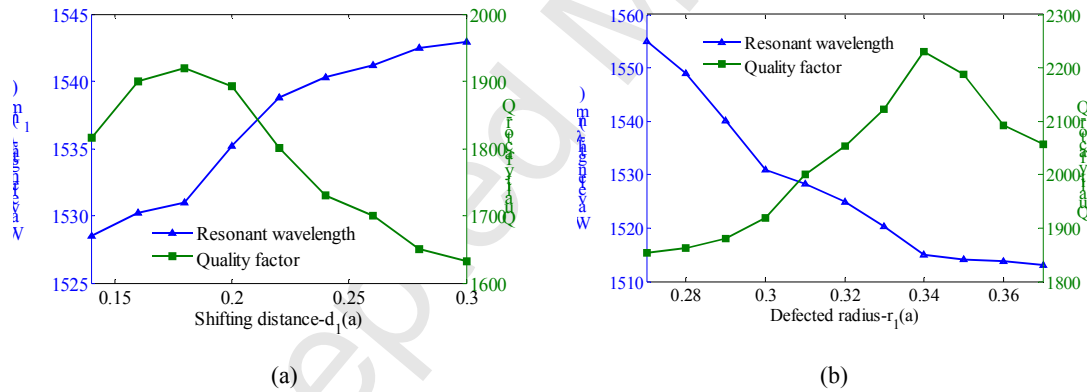


Fig. 4. Variations of resonant wavelength λ_1 and quality factor Q when the shifting distance d_1 is changed from $0.14a$ to $0.30a$ with an increment of $0.02a$ (a) and when the defected radius r_1 is changed from $0.27a$ to $0.37a$ with an increment of $0.01a$ for $d_1=0.18a$ (b).

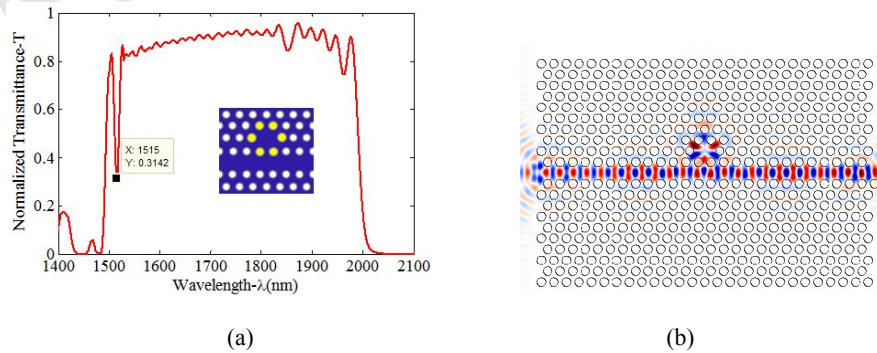


Fig. 5. Transmission spectrum (a) and electric field distribution (b) of the optimized H1 cavity with shifting distance of $0.18a$ and defected radius of $0.34a$.

3.3 RI Sensing Properties of Cascaded Cavity

As discussed above, the optimized H0 cavity and H1 cavity are integrated on a monolithic silicon substrate to form a cascaded PC cavity slab as shown in Fig. 1(b). With the final structural parameters of $a=440$ nm, $h=220$ nm, $r=132$ nm, $r_0=0.31a$, $d_0=0.22a$, $r_1=0.34a$, and $d_1=0.18a$, the composed transmission spectrum of the two cascaded PC cavities is shown in Fig. 6(a). As expected, there are two deeply narrow dips in the output transmission spectrum. Examination of Fig. 6(b) shows the electric field distribution of the fundamental TE mode that propagated in the proposed cascaded PC cavity. Each cavity has a strong optical field at corresponding defected region so that both the two PC cavities can be used for RI sensing.

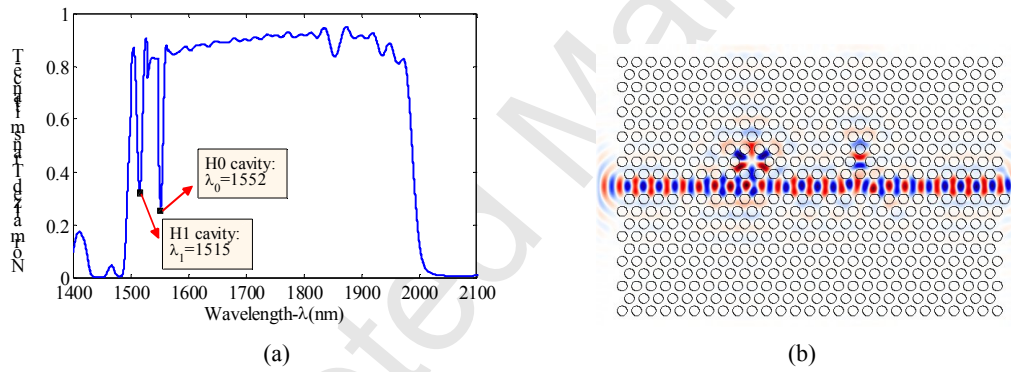


Fig. 6. Composed transmission spectrum (a) and electric field distribution (b) of two cascaded cavities.

To investigate the wavelength sensitivities of the two cascaded PC cavities to external RI, each sensor unit of PC cavity is independently subjected to RI variation of defected holes around cavity. Fig. 7(a) shows the composed transmission spectrum of the cascaded PC cavity when the H0 cavity is subjected to RI variation and the H1 cavity not, while Fig. 7(b) shows the composed transmission spectrum of the cascaded PC cavity when the H1 cavity is subjected to RI variation and the H0 cavity not. For simplicity, the RI of defected holes is only changed from 1.33 to 1.375 with an interval of 0.015. From the variation trends of two different cases, we can find that: (1) both the resonant dips of the two cavities will shift towards longer wavelength (red shift) when the

RI of any one of the two defected regions is increased; (2) if one cavity is subjected to RI disturbance, the corresponding resonant wavelength of this cavity will change obviously but the other one will only change a little, namely, the two resonant wavelengths have different shift sensitivities to RI. This allows the implementation of two individual sensors under the same condition, and eventually realizes the simultaneous measurement of two external parameters. The RI of defected holes in H0 cavity is defined as n_0 , and the RI of defected holes in H1 cavity is defined as n_1 .

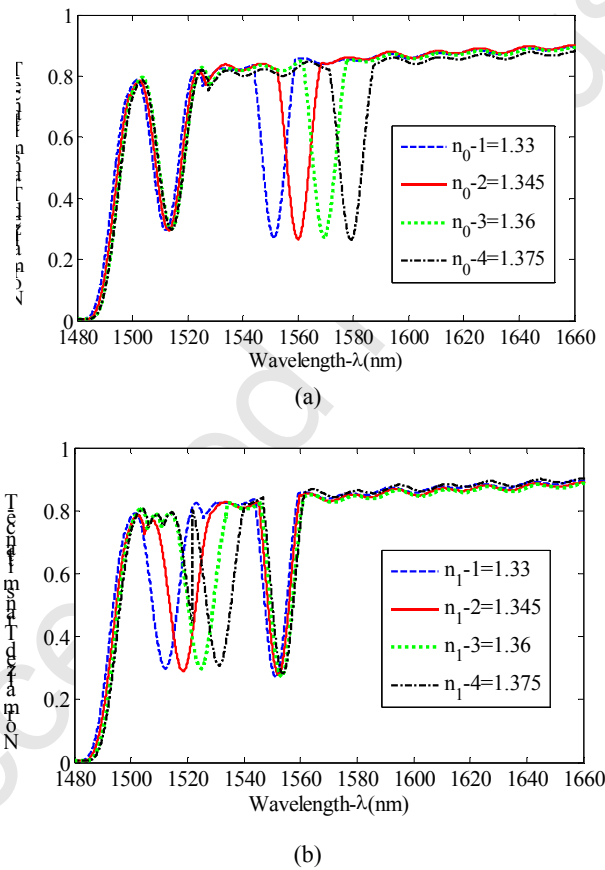


Fig. 7. Normalized transmission spectra of the cascaded PC cavity when (a) only the RI n_0 of defected holes in H0 cavity is changed and (b) only the RI n_1 of defected holes in H1 cavity is changed.

To quantitatively analyze the wavelength sensitivities of the two cascaded PC cavities to n_0 and n_1 , we calculate the shifts of the resonant wavelengths of the two cavities when n_0 and n_1 are respectively changed from 1.33 to 1.375 with an interval of 0.015. From the simulation results

shown in Fig. 8(a) and Fig. 8(b), we can get that the calculated wavelength sensitivities of the two cascaded PC cavities to n_0 are $S_{00}=620$ nm/RIU (refractive index unit) and $S_{10}=35.3$ nm/RIU, respectively; similarly, the sensitivities to n_1 are $S_{01}=55.33$ nm/RIU and $S_{11}=422$ nm/RIU, respectively. Compared with the reported refractive index sensors based on the wavelength shift of PC cavity [11], [12], whose sensitivities are respectively 235 nm/RIU and 160 nm/RIU, the sensitivities of our proposed two cavities are greatly improved.

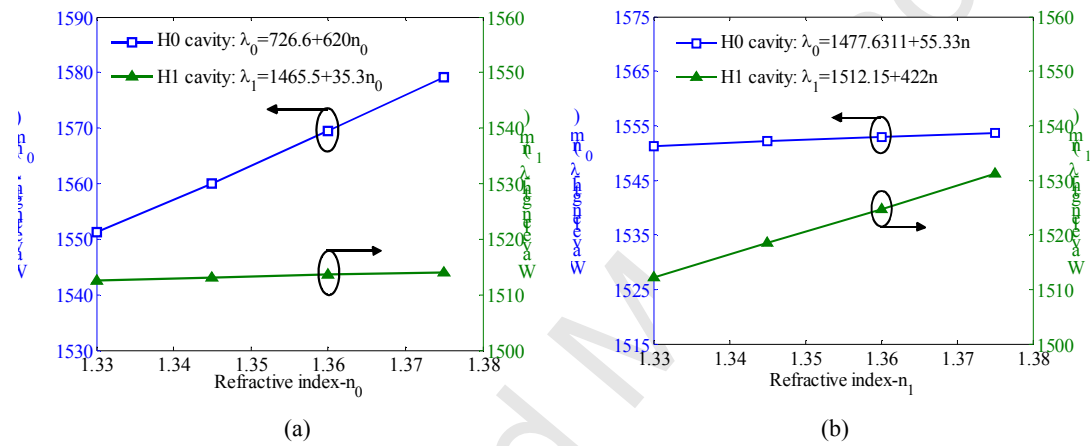


Fig. 8. Calculated wavelength sensitivities of the two cascaded PC cavities to n_0 (a) and to n_1 (b).

Then, we will investigate the crosstalk of the two cavities, which is a critical parameter for evaluating the performance of a cascaded PC cavity sensor. According to the calculation method in Ref. [31], the maximum crosstalk α can be defined as:

$$\alpha = 10 \times \lg \frac{1 - T_i}{1 - T} \quad (5)$$

where T is the minimum transmission value of one cavity sensor at the resonant wavelength λ when the corresponding RI of defected holes of this cavity is changed from 1.33 to 1.38 with an interval of 0.01; T_i is the transmission value of another cavity sensor at the same wavelength λ . Therefore, we can get the crosstalk between the proposed two cavities, as shown in Fig. 9, which demonstrates a relatively low crosstalk (lower than -6 dB).

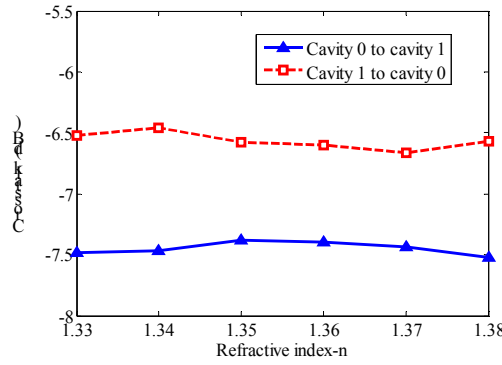


Fig. 9. Maximum crosstalk between the proposed two cascaded cavities when the RI is changed from 1.33 to 1.38 with an interval of 0.01.

4. Simulation Measurement of Liquid Concentration and Temperature

To obtain sensing properties of the proposed cascaded PC cavity in measurement of liquid concentration and temperature, the NaCl-H₂O sample with fixed concentration of 20% is adopted as the standard liquid and infiltrated in the H1 cavity, and the NaCl-H₂O solution is adopted as the measured liquid and infiltrated in the H0 cavity. According to the experimental data of the concentration-dependent and temperature-dependent refractive indices of the NaCl-H₂O sample in Ref. [22] and Ref. [25], the RI sensitivity of the NaCl-H₂O solution to concentration is considered to be $K_C = 1.71 \times 10^{-3}$ RIU/%, and the RI sensitivity of the NaCl-H₂O solution to temperature is considered to be $K_T = -1.6065 \times 10^{-4}$ RIU/K. Therefore, combining the experimental data of the NaCl-H₂O solution and the above analyzed RI sensing properties of cascaded PC cavity, we can get the relationships of wavelength shifts of two independent resonant peaks to the NaCl-H₂O concentration that need to be measured and external temperature respectively, as shown in Fig. 10(a) and Fig. 10(b). Here, the reference temperature and reference concentration of measured NaCl-H₂O solution are set as $T=300$ K and $C=0\%$, respectively. And when $T=300$ K and $C=0\%$, the resonant wavelength of H0 cavity and H1 cavity are $\lambda_0=1551.22\text{nm}$ and $\lambda_1=1526.58\text{ nm}$, respectively.

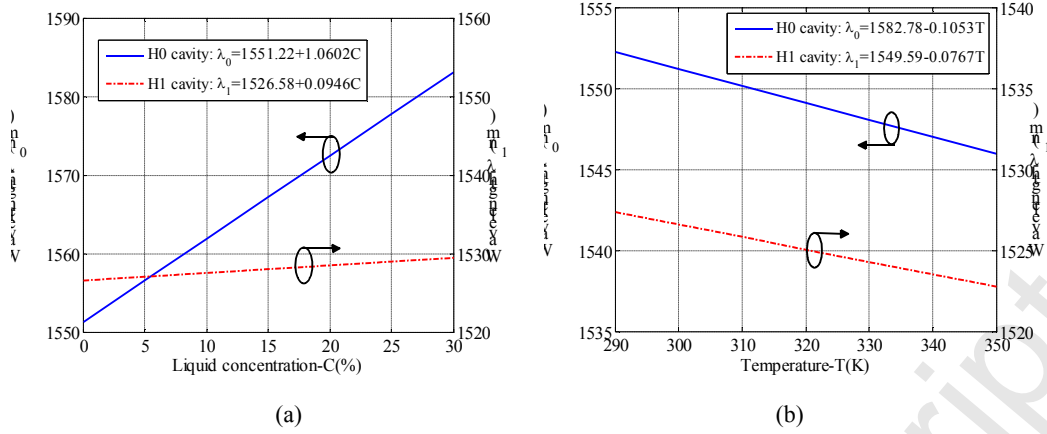


Fig. 10. Relationships of the resonant wavelengths of two cavities to NaCl-H₂O concentration that need to be measured (a) and to ambient temperature (b).

In addition, based on Eq. (3), we have:

$$\begin{pmatrix} \Delta\lambda_0 \\ \Delta\lambda_1 \end{pmatrix} = \begin{pmatrix} 1.0602 & -0.1085 \\ 0.0604 & -0.0735 \end{pmatrix} \begin{pmatrix} \Delta C \\ \Delta T \end{pmatrix} \quad (6)$$

It should be mentioned that the concentration variation ΔC of the measured NaCl-H₂O solution and temperature variation ΔT can all cause the wavelength shifts $\Delta\lambda_0$ and $\Delta\lambda_1$ of the two PC cavities. Besides, $\Delta\lambda_0$ and $\Delta\lambda_1$ have different sensitivities to ΔC and ΔT . However, when ΔC and ΔT change together, the value of ΔC and ΔT cannot be separated by only monitoring the wavelength shift of one PC cavity, as it may be generated by many different cases of ΔC and ΔT . This is also the reason why two cascaded and different PC cavities are designed in this work. As discussed above, the wavelength shift of H0 cavity $\Delta\lambda_0$ and the wavelength shift of H1 cavity $\Delta\lambda_1$ will all shift when ΔC and ΔT change together, with different shift sensitivities. Therefore, according to the dual-wavelength matrix method, ΔC and ΔT can be measured simultaneously and uniquely by monitoring $\Delta\lambda_0$ and $\Delta\lambda_1$ of the composed transmission spectrum:

$$\begin{pmatrix} \Delta C \\ \Delta T \end{pmatrix} = \begin{pmatrix} 1.0298 & -1.52 \\ 0.8462 & -14.85 \end{pmatrix} \begin{pmatrix} \Delta\lambda_0 \\ \Delta\lambda_1 \end{pmatrix} \quad (7)$$

The variation of concentration ΔC and variation of temperature ΔT can be separated by solving Eq. (7). Then, we can get the measured temperature $T = \Delta T + 300$ K and the concentration of measured NaCl-H₂O solution $C = \Delta C$. Therefore, a temperature compensated liquid concentration

sensor is also realized. The results demonstrate that the concentration and temperature sensitivities of H0 cavity are 1.0602 nm/% (red shift) and 0.0185 nm/K (blue shift), likewise, the concentration and temperature sensitivities of H1 cavity are 0.0604 nm/% (red shift) and 0.0735 nm/K (blue shift), respectively. As the minimum detectability of a current OSA could be $\Delta\lambda=1$ pm, the theoretical minimum detectable concentration and temperature could be down to 9.4322 ppm and 0.0136 K, respectively. In Ref. [21], a single-mode-multimode-single-mode fiber structure cascaded with a FBG was utilized for simultaneous measurement of liquid concentration and temperature, and the measurement sensitivity of 0.52 nm/% and 2.62 nm/K were obtained, which means that the measurement resolution of 20 ppm and 0.00038 K could be realized if the wavelength resolution of OSA is 1 pm. In Ref. [24], simultaneous measurement of refractive index and temperature with sensitivity of 90 nm/RIU and 2.36 nm/K was realized by introducing a multimode interference device inside a high birefringence fiber. In Ref. [25], simultaneous measurement of liquid concentration and temperature was obtained by measuring the Fresnel-reflection signals from the sensing heads, each of which consists of two fiber sensing tips. Then, the measurement resolution of 700 ppm and 0.35 K were realized, respectively. Compared with these sensors for simultaneous measurement of liquid concentration and temperature [21, 24, 25], the size of our proposed sensor is greatly reduced and the measurement sensitivity is well improved.

From the above analyses and designs, we can conclude that the proposed cascaded PC cavity can be well used in the simultaneous measurement of liquid concentration and temperature. Although the measurement is only performed for NaCl-H₂O solution, the proposed method can also be directly used for fast and precise measurement of concentration and temperature of any

other liquids, except that the RI sensitivities of liquid to concentration and temperature should be calibrated. In addition, although only the two cavities with resonant wavelengths of 1515 nm and 1552 nm are adopted in this study, it is possible to introduce more wavelength channels to realize quasi-distributed liquid concentration measurement. However, when considering the practical application of the proposed sensor, we should first solve two problems: one is the precise infiltration of analyte into the sensing air holes, which is the main factor of fabrication issues and determines the resonant properties of photonic crystal device; another is the capability to efficiently couple light from conventional fiber into the photonic crystal cavity. In fact, many theoretical and experimental results have demonstrated the technical feasibility to resolve the above two problems [32-35]. And we restrict the scope of this paper to the proof of the optimized cascaded PC cavity for simultaneous measurement of liquid concentration and temperature. Besides, the infiltration and coupling issues have been analyzed and designed in our previous paper [30], which are also suitable for this proposed PC cavity. Therefore, considering the space limitation, the two practical problems will not be studied in this paper.

5. Conclusions

In summary, a new technique for simultaneous measurement of liquid concentration and temperature has been demonstrated based on a PC cavity sensor with one H0 cavity and one H1 cavity cascaded together. Taking NaCl-H₂O solution as an example, standard liquid with concentration of 20% was infiltrated in defected holes of the H1 cavity, and measured liquid with undetermined concentration was infiltrated in defected holes of the H0 cavity. Both H0 cavity and H1 cavity were designed and optimized by adjusting the positions and sizes of holes around the two cavities with using FDTD simulation. For H0 cavity, the highest quality factor of 2480 at

wavelength of 1552 nm was achieved when the shifting distance was $d=0.22a$ and defected radius was $r=0.31a$. For H1 cavity, the highest quality factor of 2230 at wavelength of 1515 nm was achieved when the shifting distance was $d=0.18a$ and defected radius was $r=0.34a$. As the RI of NaCl-H₂O solution is dependent on liquid concentration and ambient temperature, we can obtain that the wavelength sensitivities of H0 cavity to the variations of measured NaCl-H₂O concentration and temperature were respectively 1.0602 nm/% (red shift) and 0.0185 nm/K (blue shift), and the wavelength sensitivities of H1 cavity to the variations of measured NaCl-H₂O concentration and temperature were respectively 0.0604 nm/% (red shift) and 0.0735 nm/K (blue shift). Furthermore, the minimum detectable NaCl-H₂O concentration of 9.4322 ppm and minimum detectable temperature of 0.0136 K were simultaneously obtained according to two-parameter matrix method.

The prominent advantages of the proposed sensor are that: (1) liquid concentration and temperature can be simultaneously obtained from the measured signal by only a sensing element and a simple signal processing method; (2) the sensor is very small (at the micron scale) and handy, which can be used for the measurement in some harsh environments and special conditions; (3) the measurement sensitivity and accuracy are attractive, and in addition, they can be further enhanced by optimizing structure of PC cavity to improve its RI sensitivity and quality factor; (4) as there are some other parameters that can induce a change of the RI of defected holes, the proposed approach also offers the possibility to integrate much more cavities on a PC slab, and to realize the simultaneous measurement of more parameters.

Acknowledgments

This work was supported in part by the National Science Foundation for Distinguished Young Scholars of China under Grant 61425003, the National Natural Science Foundation of China under Grant 61273059, the Fundamental Research Funds for the Central Universities under Grant N130104002 and N130604006, and State Key Laboratory of Synthetical Automation for Process Industries under Grant 2013ZCX09.

References:

- [1] E. S. Krueger, J. M. Baker, T. E. Ochsner, et al. On-farm environmental assessment of corn silage production systems receiving liquid dairy manure. *Journal of Soil and Water conservation*, 2013, 68(6): 438-449.
- [2] X. J. Hao, X. H. Zhou, Y. Zhang, et al. Melamine detection in dairy products by using a reusable evanescent wave fiber-optic biosensor. *Sensors and Actuators B: Chemical*, 2014, 204: 682-687.
- [3] G. Gennarelli, S. Romeo, M. R. Scarfi, et al. A microwave resonant sensor for concentration measurements of liquid solutions. *IEEE Sensors Journal*, 2013, 13(5): 1857-1854.
- [4] A. Kimoto, K. Shida. Detection of two parameters in the liquid by means of multifunctional sensing method using a pair of piezoelectric ceramics. *Sensors and Actuators A: Physical*, 2007, 134(2): 297-302.
- [5] N. Helassa, J. P. Garnett, M. Farrant, et al. A novel fluorescent sensor protein for detecting changes in airway surface liquid glucose concentration. *Biochemical Journal*, 2014, 462(2): 213-220.
- [6] Y. Zhao, Z. Q. Deng, Q. Wang. Fiber optic SPR sensor for liquid concentration measurement. *Sensors and Actuators B: Chemical*, 2014, 192: 229-233.
- [7] T. K. Yadav, R. Narayanaswamy, M. H. Abu Bakar, et al. Single mode tapered fiber-optic interferometer based refractive index sensor and its application to protein sensing. *Optics*

- Express, 2014, 22(19): 22802-22807.
- [8] G. L. Yin, S. Q. Lou, H. Zou. Refractive index sensor with asymmetrical fiber Mach-Zehnder interferometer based on concatenating single-mode abrupt taper and core-offset section. *Optics & Laser Technology*, 2013, 45: 294-300.
- [9] M. Notomi. Strong light confinement with periodicity. *Proceedings of the IEEE*. 2011, 99(10): 1768-1779.
- [10] P. Lalanne, C. Sauvan, J. P. Hugonin. Photon confinement in photonic crystal nanocavities. *Laser & Photonics Reviews*. 2008, 2(6): 514-526.
- [11] C. Caer, S. F. Serna-Otalvaro, W. W. Zhang, et al. Liquid sensor based on high-Q slot photonic crystal cavity in silicon-on-insulator configuration. *Optics Letters*, 2014, 39(20): 5792-5794.
- [12] L. J. Huang, H. P. Tian, J. Zhou, et al. Label-free optical sensor by designing a high-Q photonic crystal ring-slot structure. *Optics Communications*, 2015, 335: 73-77.
- [13] E. Chow, A. Grot, L. W. Mirkarimi, et al. Ultracompact biochemical sensor built with two-dimensional photonic crystal microcavity. *Optics Letters*, 2004, 29(10): 1093-1095.
- [14] P. P. Xu, K. Y. Yao, J. J. Zheng, et al. Slotted photonic crystal nanobeam cavity with parabolic modulated width stack for refractive index sensing. *Optics Express*, 2013, 21(22): 26908-26913.
- [15] F. L. Hsiao, C. Lee. Computational study of photonic crystals nano-ring resonator for biochemical sensing. *IEEE Sensors Journal*, 2010, 10(7): 1185-1191.
- [16] W. C. Lai, S. Chakravarty, Y. Zou, et al. Silicon nano-membrane based photonic crystal microcavities for high sensitivity bio-sensing. *Optics Letters*, 2012, 37(7): 1208-1210.
- [17] S. Pal, A. R. Yadav, M. A. Lifson, et al. Selective virus detection in complex sample matrices with photonic crystal optical cavities. *Biosensors & Bioelectronics*, 2013, 44: 229-234.
- [18] Y. Zou, S. Chakravarty, D. N. Kwong, et al. Cavity-waveguide coupling engineered high sensitivity silicon photonic crystal microcavity biosensors with high yield. *IEEE Journal of Selected Topics in Quantum Electronics*, 2014, 20(4): 6900710.
- [19] J. Harris, P. Lu, H. Larocque, et al. In-fiber Mach-Zehnder interferometric refractive index sensors with guided and leaky modes. *Sensors and Actuators B: Chemical*, 2015, 206: 246-251.

- [20] Y. Zhao, Y. N. Zhang, R. Q. Lv. Simultaneous measurement of magnetic field and temperature based on magnetic fluid-infiltrated photonic crystal cavity. *IEEE Transactions on Instrumentation and Measurement*, 2014, in publish.
- [21] Y. Zhao, L. Cai, X. G. Li, et al. Liquid concentration measurement based on SMS fiber sensor with temperature compensation using an FBG. *Sensors and Actuators B: Chemical*, 2014, 196: 518-524.
- [22] L. V. Nguyen, M. Vasiliev, K. Alameh. Three-wave fiber fabry-pérot interferometer for simultaneous measurement of temperature and water salinity of seawater. *IEEE Photonics Technology Letters*, 2011, 23(7): 450-452.
- [23] D. A. C. Enriquez, A. R. da Cruz, M. T. M. R. Giraldi. Hybrid FBG-LPG sensor for surrounding refractive index and temperature simultaneous discrimination. *Optics & Laser Technology*, 2012, 44(4): 981-986.
- [24] C. Gouveia, G. Chesini, C. M. B. Cordeiro, et al. Simultaneous measurement of refractive index and temperature using multimode interference inside a high birefringence fiber loop mirror. *Sensors and Actuators B: Chemical*, 2013, 177: 717-723.
- [25] J. R. Zhao, X. G. Huang, J. H. Chen. A Fresnel-reflection-based fiber sensor for simultaneous measurement of liquid concentration and temperature. *Journal of Applied Physics*, 2009, 106(8): 083103.
- [26] D. Q. Yang, H. P. Tian, N. N. Wu, et al. Nanoscale torsion-free photonic crystal pressure sensor with ultra-high sensitivity based on side-coupled piston-type microcavity. *Sensors and Actuators A: Physical*, 2013, 199: 30-36.
- [27] S. Olyaei, S. Najafgholinezhad. A high quality factor and wide measurement range biosensor based on photonic crystal nanocavity resonator. *Sensor Letters*, 2013, 11: 483-488.
- [28] A. F. Oskooi, D. Roundy, M. Ibanescu, et al. Meep: A flexible free-software package for electromagnetic simulations by the FDTD method. *Computer Physics Communications*, 2010, 181(3): 687-702.
- [29] J. Li, T. P. White, L. O'Faolain, et al. Systematic design of flat band slow light in photonic crystal waveguides. *Optics Express* 2008, 16(9): 6227-6232.
- [30] Y. N. Zhang, Y. Zhao, Q. Wang. Multi-component gas sensing based on slotted photonic crystal waveguide with liquid infiltration. *Sensors and Actuators B: Chemical*, 2013, 184:

179-188.

- [31] D. Q. Yang, H. P. Tian, Y. F. Ji. Nanoscale low crosstalk photonic crystal integrated sensor array. *IEEE Photonics Journal*, 2014, 6(1): 4200107.
- [32] H. H. J. E. Kicken, P. F. A. Alkemade, R. W. van der Heijden, et al. Wavelength tuning of planar photonic crystals by local processing of individual holes. *Optics Express*, 2009, 17(24): 22005-22011.
- [33] C. L. C. Smith, D. K. C. Wu, M. W. Lee, et al. Microfluidic photonic crystal double heterostructures. *Applied Physics Letters*, 2007, 91: 121103.
- [34] Y. Chau, T. Yang, W. Lee. Coupling technique for efficient interfacing between silica waveguides and planar photonic crystal circuits. *Applied Optics*, 2004, 43(36): 6656-6663.
- [35] A. Hosseini, X. Xu, D. N. Kwong, et al. On the role of evanescent modes and group index tapering in slow light photonic crystal waveguide coupling efficiency. *Applied Physics Letters*, 2011, 98: 031107.

Biography:

Yong Zhao received his M.A. and Ph.D. degrees, respectively, in precision instrument & automatic measurement with laser and fiber-optic techniques from the Harbin Institute of Technology, China, in 1998 and 2001. He was awarded a first prize scholarship in 2000 by the China Instrument and Control Society and the Sintered Metal Corporation (SMC) scholarship in Japan. He was a scholarship in Japan. He was a postdoctor in the Department of Electronic Engineering of Tsinghua University from 2001 to 2003, and then worked as an associate professor in the Department of Automation, Tsinghua University of China. In 2006, he was a visiting scholar of University of Illinois in Urbana and Champagne, USA. In 2008, he was awarded as the “New Century Excellent Talents in University” by the Ministry of Education of China. In 2009, he was awarded as the “Liaoning Bai-Qian-Wan Talents” by Liaoning Province. In 2011, he was awarded by the Royal Academy of Engineering as an academic researcher of City University London. He was awarded by the National Science Foundation for Distinguished Young Scholars of China, in 2014. Now he is working in Northeastern University as a full professor. As a leader of his research group, his current research interests are the development of fiber-optic sensors and device, fiber Bragg grating sensors, novel sensor materials and principles, slow light and sensor technology, optical measurement technologies. He has authored and co-authored more than 180 scientific papers and conference presentations, 7 patents, and 4 books. He is a member in the Editorial Boards of the international journals of Sensor Letters, Instrumentation Science & Technology, Journal of Sensor Technology, and Advances in Optical Technologies.



Ya-nan Zhang was born in Anhui, China, in June 1989. She received her B.A. and M.A. degrees, respectively, in 2010 and 2012 from the College of Information Science and Engineering, Northeastern University, Shenyang, China, where she is currently working toward the Ph.D. degree. Her research interests include fiber optical sensors, photonic crystal waveguide sensors, and slow light technology and its sensing applications. She has authored and co-authored more than 20 scientific papers and 5 patents.



Hai-feng Hu was born in Liaoning, China, in 1984. He received his Ph.D degrees in the Institute of Semiconductors, Chinese Academy of Sciences, China, in 2013. He is currently working in the College of Information and Engineering at Northeast University. His research interests are nano-optics, plasmonics, fiber-optic sensors and their applications in biosensing. He has authored and co-authored more than 20 scientific papers, 2 patents and 5 conference presentations.